Mechanics & Industry **19**, 503 (2018)
© AFM, EDP Sciences 2018
https://doi.org/10.1051/meca/2017064

Mechanics & Industry

Available online at:
www.mechanics-industry.org

Regular Article

Thermal characterization of a plate heated by a multi-jet system

Amar Zerrout*, Ali Khelil, and Larbi Loukarfi

Control Laboratory, Test, Measurement and Mechanical Simulation, University of Chlef, Algeria B.P. 151, 02000 Chlef, Algeria

Received: 11 May 2017 / Accepted: 22 December 2017

Abstract. This study is an experimental and numerical analysis of the influence from changes in the conditions of inputs temperature and velocity on the behavior thermal and dynamic of a multi-jet swirling system impacting a flat plate. The experimental device comprising three diffusers arranged in line, of diameter D aloof $2D$ between the axes of their centers, impinging the plate perpendicularly at an impact height $H = 6D$. The swirl is obtained by a generator (swirl) of composed 12 fins arranged at 60° relative to the vertical placed just at the exit of the diffuser. By imposing the temperature and velocity for three input conditions with three studied configurations. The paper deals with find the configuration that optimizes the best thermal homogenization. The results show that the configuration having an equilibrated inlet temperature (T, T, T) is derived from a good temperature distribution on the baffle wall and a better thermal transfer from the plate. The system was numerically simulated by the fluent code by using the turbulence model (k–ε). This last has yielded results accorded to those experimental results.

Keywords: Impinging swirling jet / multiple jet / thermal homogenization / plane plate / (k-ε) model

1 Introduction

Several industrial techniques engender impinging jets in the areas of industry. They are commonly used for cooling process, heating or drying, such as drying of paper and textiles, electronics cooling, cooling of gas turbine blades, cooling the glass sheets, cooling of combustion chambers of new generation and processing of the polymers, in the aim of optimizing heat transfer between a fluid and a structure. Several experimental and numerical works have shown the possibility to improve the heat transfer by the implementation of the impact of jets. Despite the number of jobs on the impacting jets, there are very few systematic studies of quantization the mixing layer. Still we can cite the work of Ding et al. [1] in jet impacting small distance ($y/d < 5$). Their analysis focuses particularly on the wall jet region after impact. These jet types are notably used for heat exchange. In fact, the optimal distance to cool a surface is at the place where the intensity of the axial turbulence reaches a maximum. This maximum is localized to h/d comprised between 6 and 8. This explains that the impacting jets are usually studied for impact distance h smaller than 10 diameters (Fig. 1).

2 Experimental configuration

The realized experimental device consists of a frame of the cubic form of metal with dimensions (1.20 m × 1, 20 × 2, 0 m); having at its upper part the devices for blowing hot air (hair dryer), directed from the top down to the bottom and different types of diffusers (1) depending on the configuration studied part. This device allows to scan the maximum space provided by a particular arrangement of the rods supporting the thermal sensors (2); the temperature field is explored with a portable anemometer unit VELOCICALC more (4). The probe rods are easily guided vertically and horizontally by supports to scan the maximum space, a horizontal plate (3) material Formica. The ambient temperature Ta is obtained by a digital thermometer (5) from the measurements of temperature T in different parts of the jet. The temperature at the origin blowing T_{max} is raised for each type and configuration of the jet (Fig. 2).

3 The number of swirl

The swirl number of adding an azimuthally component to the velocity field of the result is a flow, the swirl makes coherent structure, strongly held in the case of the free jet lower suppressing vortex-pairing (pairing of vortices) and by an increase of the turbulence. It was observed that as of a certain intensity of the onset of the swirl zone in the main

* e-mail: zerroutamar@yahoo.fr

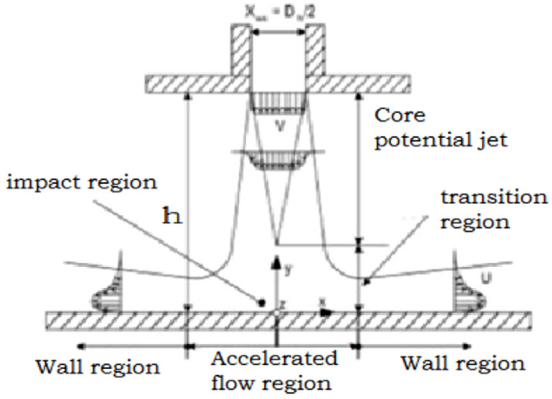

Fig. 1. Different characteristic regions of impinging transitional jet, Rady and Arquis [2].

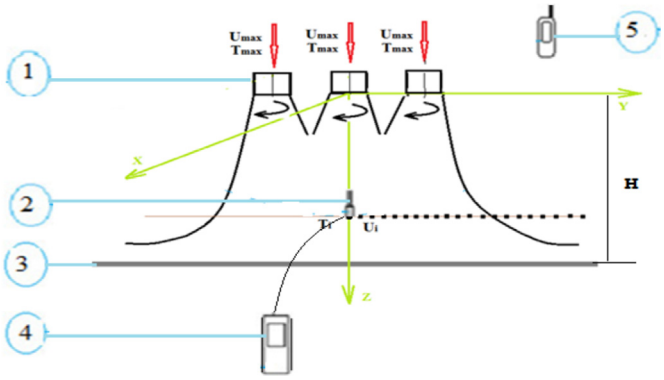

Fig. 2. Experimental facility and test assembly, Zerrout [3].

flow recirculation. The vortex generated by the swirl effect to make the anisotropic turbulence, it has an inhibitory effect on the transfer of energy from large organizations to small structures. The swirl is characterized by a dimensionless number that defines a measure of the ratio between the angular momentum of the axial flow G_θ and axial flow of the axial momentum G_X (axial thrust) Gupta et al. [4].

$$S = \frac{G_\theta}{RG_X} = \frac{\int_0^R r^2 UW dr}{R\int_0^R r\left(U^2 - \frac{W^2}{2}\right)dr}. \quad (1)$$

The swirl number can be evaluated at any position of the jet because the two quantities are calculated. Swirling helps promote and improve the process of mixing and transfer, as well as the jet has the advantage of quickly flourish in free jets.

Another empirical formula is used for calculating the number of swirl that the swirl number defined according to the geometric parameters of the swirl generator. This number S can be written as Hung et al. [5] as follows:

$$S = \frac{2}{3}\left[\frac{1-\left(\frac{R_h}{R_n}\right)^3}{1-\left(\frac{R_h}{R_n}\right)^2}\right]\cdot tg\alpha. \quad (2)$$

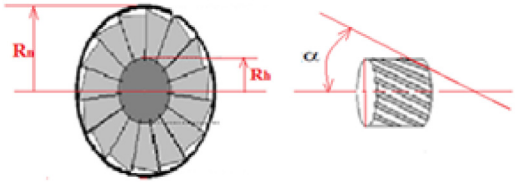

Such that: α is the angle of the fins built swirl generator, R_h the radius of the vane diffuser support, and R_n is the radius of diffuser.

It will be noted that in the case of a swirler without hub ($R_h = 0$), the expression becomes: Sato et al. [6].

$$S = \frac{2}{3}tg\alpha, \quad (3)$$

4 Operating conditions

The experimental setup was placed in a local having the following dimensions: length = 4 m, width = 3.5 m and height = 3 m. There must be a free flow of the isolation and testing, the initial temperature at the blowing diffuser was 90 °C for each jet.

5 Measurement procedure

The values of the initial temperature T_i and the flow value of the ambient temperature T_a measured by the temperature sensors of precision (1/100). They are raised until the temperature stabilizes. The ten minute delay was sufficient to achieve this stabilization, after measuring, the temperatures for a given configuration, and the pairs of blowing is stopped and the movement of the rods proceeds door sensors to other measurement point.

6 Dimensionless parameters

The reduced temperature (T_r) of measurement is obtained by reference to the maximum average temperature at the outlet of the blowing opening and at room temperature:

$$T_r = \frac{T_i - T_a}{T_{\max} - T_a}. \quad (4)$$

Reduced dimensionless axial velocity is obtained with respect to the maximum velocity at the outlet of the blowing port.

$$U_r = \frac{U_i}{U_{\max}}. \quad (5)$$

Similarly, the azimuthal and axial distances are given by reference to the diameter of the blowing diffuser in dimensionless form y/D.

The accuracy for the calibration of the temperature is at least 6:1 in accordance with the characteristics of the precision of the calibrated devices. The accuracy for the calibration of the pressure is at least the ratio 2.5:1 in

Table 1. Showing different types of diffusers, entry conditions of temperature and velocity.

Configurations	Number of outlet jets	Temperature distribution	Velocity distribution	Height of impact
Configuration (a)	3	$(T,\ T,\ T)$	$(U,\ U,\ U)$	$6D$
Configuration (b)	3	$(T,\ T/2,\ T)$	$(U,\ U/2,\ U)$	$6D$
Configuration (c)	3	$(T/2,\ T,\ T/2)$	$(U/2,\ U,\ U/2)$	$6D$

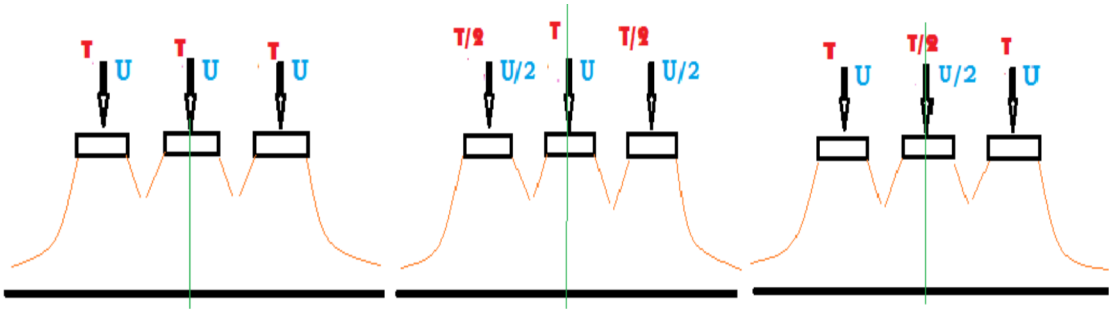

Fig. 3. Different types of diffuser.

accordance with the characteristics of the precision of the calibrated devices. The accuracy for the calibration of the velocity is at least 1:1 in accordance with the characteristics of the precision of the calibrated devices. The results of the calibration tests of the anemometer portable device Velocecalc Plus more are percentages of tolerance which the temperature is ±0.3 °C of reading, the pressure is ±1.0% of reading, velocity is ±3% of reading.

7 Heat transfer from the impinging jets

The heat transfer from the impinging jets is characterized by the Nusselt number. It is a dimensionless number that quantifies the heat transfer between a fluid and a wall of the baffle plate. It represents the ratio of convective exchanges on conductive exchanges Wigley and Clark [7].

With:

$$Nu = \frac{h \cdot L}{\lambda}, \tag{6}$$

where h is the local convective heat transfer coefficient [W m^{-2} K^{-1}], λ the thermal conductivity of air, taken at the reference temperature [W m^{-1} K^{-1}], and L is the length of the plate [m].

According to Murray et al. [8] for a turbulent flow, the Nusselt number is calculated by an empirical formula:

$$Nu = 0.042 \cdot (Re)^{0.8} \cdot (Pr)^{0.33}, \tag{7}$$

Re is the Reynolds number. It is defined by:

$$Re = \frac{\rho \cdot U \cdot L}{\mu}, \tag{8}$$

ρ is the density of air, U the average velocity [m s^{-1}], and Pr is the Prandtl number is a dimensionless number; it represents the ratio of momentum diffusivity and thermal diffusivity

$$Pr = \frac{\mu \cdot Cp}{\lambda}, \tag{9}$$

μ is the dynamic viscosity [N s m^{-2}], C_p the specific heat [J kg^{-1} K^{-1}], λ is the air thermal conductivity en [W m^{-1} K^{-1}]

8 The different types of diffusers

See Table 1 and Figure 3.

9 Numerical procedure

The turbulence model (k–ε) is a turbulent viscosity model in which Reynolds stresses are assumed to be proportional to the average velocity gradients, with a proportionality constant representing turbulent viscosity.

This hypothesis, known as the "Boussinesq" hypothesis, provides the following expression for the Reynolds stress tensor, Launder et al. [9].

$$\rho \overline{u'_i u'_j} = \rho \frac{2}{3} k \delta_{ij} - \mu_t \left(\frac{\partial u_i}{\partial x_j} + \frac{\partial u_j}{\partial x_i} \right) + \frac{2}{3} \mu_t \frac{\partial u_i}{\partial x_i} \delta_{ij}, \tag{10}$$

k is the turbulent kinetic energy defined by:

$$k = \frac{1}{2} \sum_i \overline{u'^2_i}. \tag{11}$$

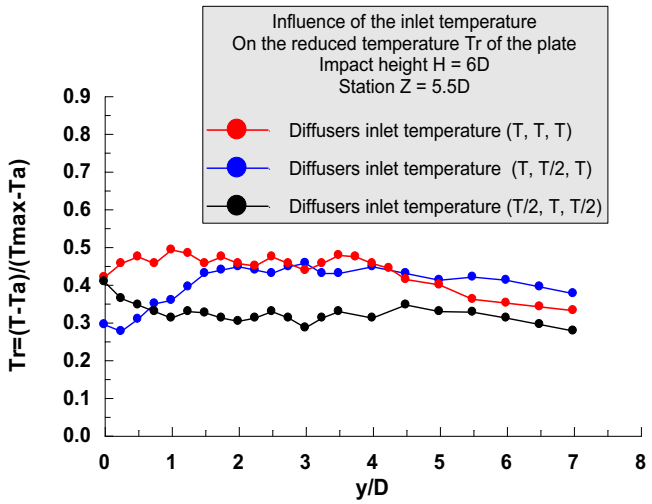

Fig. 4. Influence of disequilibrium in temperatures at the inlet diffusers on the temperature of the plaque with height of impact $H=6D$ and station $Z=5.5D$.

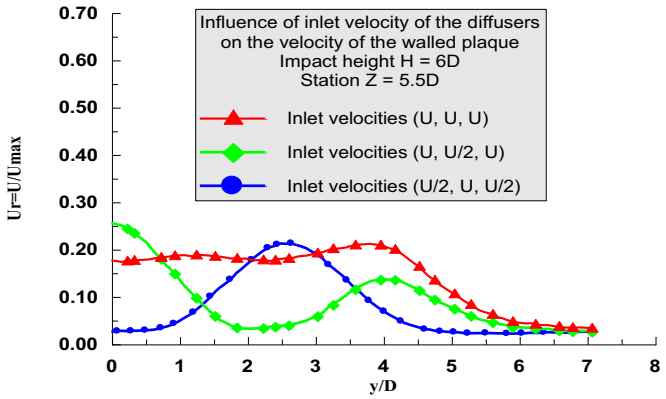

Fig. 5. Influence of disequilibrium in velocity at the inlet of the diffusers on the velocity of wall of the plate with impact height $H=6D$ and station $Z=5.5D$.

The turbulent viscosity is obtained by assuming that it is proportional to the product of the scale of the turbulent velocity and the scale of length. In the model (k–ε), these scales of velocities and lengths are obtained from two parameters, the kinetic energy k and the rate of dissipation ε. Thus can be expressed by the following relation:

$$\mu_t = \rho C_\mu \frac{k^2}{\varepsilon}, \tag{12}$$

with $C_\mu = 0.09$ is the empirical constant.

The values of k are required in the equation are obtained by solving the following conservation equation:

$$\frac{\partial}{\partial t}(\rho k) + \frac{\partial}{\partial x_i}(\rho u_i k) = \frac{\partial}{\partial x_j}\left[\left(\mu + \frac{\mu_t}{\sigma_k}\right)\frac{\partial k}{\partial x_j}\right] + G_k + G_b - \rho\varepsilon + S_k$$

$$\frac{\partial}{\partial t}(\rho\varepsilon) + \frac{\partial}{\partial x_i}(\rho u_i \varepsilon) = \frac{\partial}{\partial x_j}\left[\left(\mu + \frac{\mu_t}{\sigma_k}\right)\frac{\partial \varepsilon}{\partial x_j}\right] + C_{1\varepsilon}\frac{\varepsilon}{k}(G_k + C_{3\varepsilon}G_b) - C_{2\varepsilon}\rho\frac{\varepsilon^2}{k} + S_\varepsilon, \tag{13}$$

with $C_{1\varepsilon} = 1.44$ and $C_{2\varepsilon} = 1.92$; Empirical constants. $\sigma_k = 1.0$ and $\sigma_\varepsilon = 1.3$ the Prandtl numbers for k and ε, respectively. S_k and S_ε are the source terms for k and ε, respectively. G_k represents the generation of the turbulent kinetic energy due to the gradient of the average velocities.

$$G_k = \mu_t\left(\frac{\partial u_j}{\partial x_i} + \frac{\partial u_i}{\partial x_j}\right)\frac{\partial u_j}{\partial x_i}, \tag{14}$$

G_b is the coefficient of generation of turbulence due to training

$$G_b = -g_i\frac{\mu_t}{\rho\sigma_h}\frac{\partial \rho}{\partial x_i}. \tag{15}$$

9.1 Computational domain and mesh

For numerical simulation of this type of flow, mesh generation was carried out with tetrahedral meshes comprising 1 201 672 cells. Calculations were tested on different meshes up to 1 547 214 cells for the control of the solution, in order to seek the limit of the independence of the solution with respect to the fineness of the mesh [10], it was found that the solution has not been changed. We can therefore conclude that the mesh is acceptable and the solution is independent of the mesh.

10 Results and discussion

10.1 Influence of entry conditions on the temperature of the plate

Figure 4 shows the temperature profiles for the resorts near the impact ($Z=3.5D$). These curves clearly show the influence of inlet temperatures conditions of diffusers ($T/2$, T, $T/2$), (T, $T/2$, T) and (T, T, T), on the reduced temperature wall.

It is noticed that the promoter which has temperatures equilibrated at the inlet (T, T, T) gives a more uniform temperature distribution on the surface of the plate relative to those of other configurations. This homogenization of the temperature drifts of a better heat transfer from the plaque.

10.2 On the reduced average velocity *Ur*

Figure 5 shows three numerical curves for three configurations velocity distribution to the input of diffusers (U, U, U), (U, $U/2$, U), ($U/2$, U, $U/2$) by setting the measuring station $Z=3.5D$, with $H=$ height of impact $6D$.

It is found that the speed is more balanced to the input; the greater will be velocity stability and becomes an almost uniform over the entire surface of the plate. We conclude that the velocity stabilization is obtained for multiple jets impinging transitional ($H=6D$), having uniform entry flow velocity's of.

10.3 On the Nusselt number *Nu*

Figure 6 shows the superposition of three numerical curves of the variation of Nusselt number Nu, depending on the ratio of the radial distance dimensionless y/D for an impact height $H=4D$, setting a station near the impact wall $Z=3.5D$.

The profiles are compared for three respective input conditions of temperature (T, T, T), (T, $T/2$, T), ($T/2$, T, $T/2$). Is noticed that the configuration having a temperature distribution (T, T, T) gives a number of good Nusselt moderate compared than that of other configurations of input temperatures. So, the more we balance the temperature and velocity at the inlet greater the number Nusselt stabilizes and becomes a moderated to impact wall, which better promotes convective transfer of the plate.

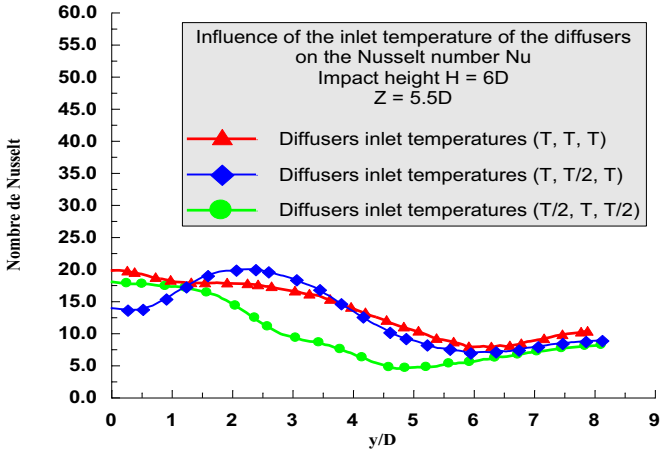

Fig. 6. Influence of the inlet temperature of the diffusers on the profiles of the Nusselt number to the wall with impact of height $H=6D$ and station $Z=3.5D$.

10.4 On the temperature field

Figure 7 shows the contour temperature fields T on the wall of the plate of a system of three jets impacting the plate at a height $H=6D$, respectively, for the inlet temperatures to the diffuser (T, T, T), ($T/2$, T, $T/2$) and (T, $T/2$, T). It is noted that in Figure 7a, the distribution of the temperature field is uniformly distributed over the whole domain with respect to the other configurations (b) and (c). The temperature reaches the entire surface of the plate, thus promoting the homogeneity of the heat transfer over the entire surface of the plate.

11 Validation of the results

The comparison of numerical and experimental results is evidenced in Figure 8a–c, relating to the reduced temperature T_r, the reduced velocity Ur and Nusselt number Nu in the plan (y, z), respectively.

The numerical results of the model with two transport equations (k–ε) used to simulate the present case are in good agreement with experimental results. Notwithstanding some shortcomings of this model (k–ε), he gave acceptable results qualitatively. It is nevertheless a tool of simulation relatively simple to use and inexpensive.

12 Conclusion

An experimental study and a numerical simulation of a multiple swirling jet system impinging a plane plate have summers realized.

By characterizing the behavior of the thermal and dynamic field of flow configurations studied, we note that:
– The multiple jets ensure more mixing homogenization with a larger spreading.

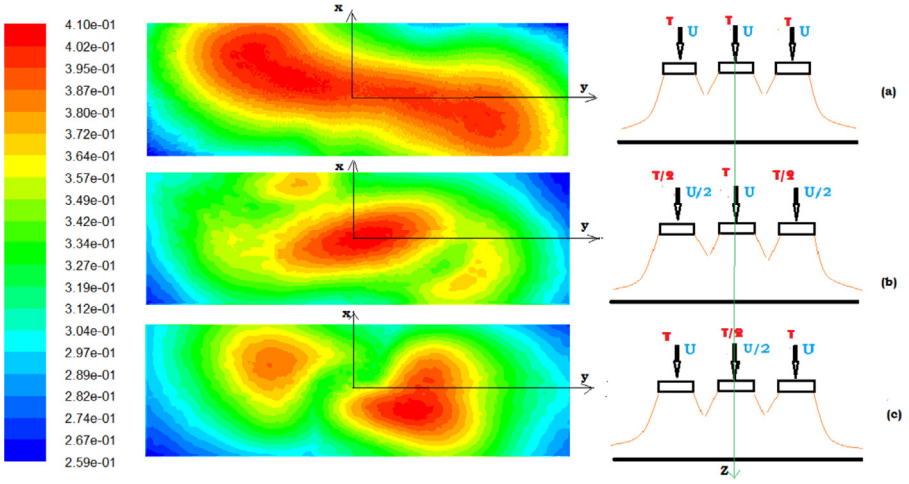

Fig. 7. Contour temperature field of the plaque at height of impact $6D$.

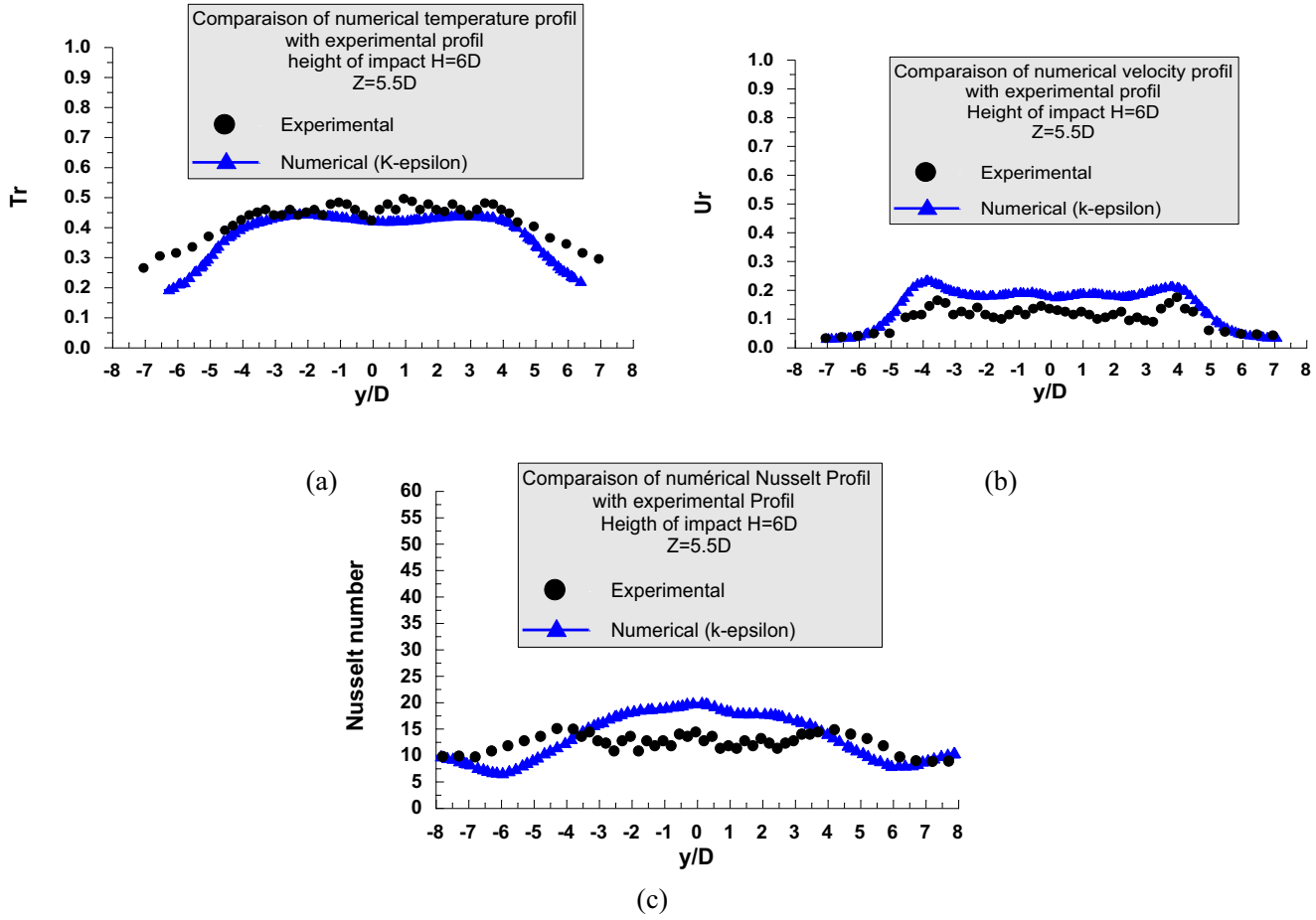

Fig. 8. Comparison of numerical and experimental profiles, (a) the reduced temperature T_r, (b) the reduced speed Ur, (c) the Nusselt number Nu, for station $Z = 5.5D$ with high impact $H = 6D$, and inlet temperatures is (T, T, T) in the plan (y, z).

– The diffusers having the configuration (T, T, T), ensuring a uniform temperature distribution over the entire surface of the plate and a good thermal homogenization.

In the configurations ($T/2$, T, $T/2$) and (T, $T/2$, T) after diffusion of the jets, the temperature contours reach the whole surface of the plate, with respect to the configuration (T, T, T).

– The more we balance the temperature and velocity at the entry, the more we obtain a uniform and moderate the temperature of the plate is heated.
– The numerical results and the experimental results presented in this study indicate that the model with two transport equations (k–ε) is best suited for this type of flow. Also it remains a relatively simple simulation tool to use and inexpensive.
– These configurations of swirling multijet allow a perfect distribution of the jets with a homogenization of the heat transfer the plate.

This mixing ratio may be influenced by other parameters, such as the swirl direction of the central jet, the inclination of the axes of side jets, the variation of the center distance, the geometry diffusers, etc. These will be examined in a forthcoming study.

Nomenclatures

D	Nozzle diameter, m
d	Support vane diameter, m
G_θ	Angular momentum flux, kg m^2 s^{-2}
G_X	Axial momentum flux, kg m^2 s^{-2}
H	Impacting height, m
h	Local convective heat transfer coefficient, W m^{-2} K^{-1}
k	Kinetic energy of turbulence, m^2 s^{-2}
L	Length of the plate
Nu	Nusselt number
R	Diffuser radius, m
S	Swirl number
R_h	Support vane diameter, m
R_n	Diffuser radius, m
Re	Reynolds number
T_a	Ambient temperature, °C
T_i	Jet temperature at the point considered, °C.
T_{max}	Maximum temperature at the diffuser exit, °C
T_r	Dimensionless temperature
U	Axial mean velocity, m s^{-1}
U_{max}	Maximum velocity at the diffuser exit, m s^{-1}
U_r	Dimensionless axial velocity
V	Radial velocity, m s^{-1}
W	Tangential velocity, m s^{-1}

Greek symbols

λ The thermal conductivity of air, W m^{-1} K^{-1}
α Angle of the fins built swirl generator
C_μ Empirical constant
σ_t Prandtl numbers for kinetic energy of turbulence
δ_{ij} Tensor identity
ε The rate of dissipation of kinetic energy, m^2 s^{-2}
μ_t Turbulent viscosity, kg m^{-1} s^{-1}
μ Dynamic viscosity, N s m^{-2}
C_p Specific heat, J kg^{-1} K^{-1}
ρ Density of air, kg m^{-3}

References

[1] R. Ding, J. Revstedt, L. Fuchs, Study of mixing in circular impinging jets – effects of boundary conditions, Proceedings of PSFVIP-4, June 3–5, Chamonix (France), 2003
[2] M. Rady, E. Arquis, Heat transfer enhancement of multiple impinging slat jets, with symmetric exhaust ports and confinement surface protrusion, Appl. Therm. Eng. 26 (2005) 1310–1319
[3] A. Zerrout, Experimental and numerical study of a swirling impacting multiple jet system, PhD Thesis in Science, Genie-Mechanical Specialty, Faculty of Technology, University of Chlef, Algeria, 2016
[4] A.K. Gupta, D.G. Lilley, N. Syred, Swirl Flows, Abacus Press, London, 1984
[5] Y. Huang, V. Yang, Dynamics and stability of lean-premixed swirl-stabilized combustion, Prog. Energy Combust. Sci. 35 (2009) 293–364
[6] H. Sato, M. Mori, T. Nakamura, Development of a dry ultra-low NOx double swirler staged gas turbine combustor, J. Eng. Gas Turbines Power 120 (1998) 41–47
[7] G. Wigley, J.A. Clark, Heat transport coefficients for constant energy flux models of broad leaves, Boundary Layer Meteorol. 7 (1974) 139–150
[8] D. Murray, P.S. Myers, O.A. Uyehara, Proceedings of the International Heat Transfer Conference, 1966, Vol. 2, p. 292
[9] B.E. Launder, D.B. Spalding, The numerical computation of turbulent flows, Comput. Methods Appl. Mech. Eng. 3 (1974) 269–289
[10] FLUENT User's Guide, 2006

Cite this article as: A. Zerrout, A. Khelil, L. Loukarfi, Thermal characterization of a plate heated by a multi-jet system, Mechanics & Industry **19**, 503 (2018)